

Design, Synthesis and Biological Evaluation of Pyridin-3-yl pyrimidines as Potent Bcr-Abl Inhibitors

Xiaoyan Pan, Jinyun Dong, Hongping Gao, Fang Wang, Yanmin Zhang, Sicen Wang and Jie Zhang*

School of Medicine, Xi'an Jiaotong University, No. 76, Yanta West Road, Xi'an 710061, China

*Corresponding author: Jie Zhang, zhj8623@mail.xjtu.edu.cn

A series of pyridin-3-yl pyrimidines was synthesized and evaluated for their Bcr-Abl inhibitory and anticancer activity. The preliminary results indicated that some compounds were promising anticancer agents. Compounds A2, A8, and A9 exhibited potent Bcr-Abl inhibitory activity, suggesting that aniline containing halogen substituents might be important for biological activity. Molecular docking was carried out to investigate the binding mode of them with Bcr-Abl. Details of synthesis and SAR studies of these compounds are described.

Key words: 3D-QSAR, anticancer, Bcr-Abl, leukemia cell, pyridin-3-yl pyrimidines

Received 12 March 2013, revised 5 October 2013 and accepted for publication 5 December 2013

Recent advances in cancer therapy afford molecular targeting agents with high efficiency and low toxicity (1). Chronic myelogenous leukemia (CML) is hematological malignancy caused by chromosomal rearrangement that generates Bcr-Abl. Bcr-Abl is a fusion protein with deregulated tyrosine kinase activity, which is essential for pathogenesis of CML (2). It is regarded as highly attractive target for drug intervention. Bcr-Abl inhibitors are the first-line therapy for most patients with CML.

Nilotinib is a potent Bcr-Abl inhibitor for the treatment for CML (3). Crystallographic studies revealed that it could stabilize the inactive conformation of Bcr-Abl (4). Nilotinib interacts with Bcr-Abl through four key interactions: hydrogen-bond interactions with hinge region, hydrophobic interactions with gatekeeper region, hydrogen-bond interactions with DFG motif, and hydrophobic interactions with allosteric region (Figure 1) (5).

Nilotinib could fit into the kinase domain of Bcr-Abl, which was quite conserved. The allosteric region, which was adjacent to ATP-binding site, was considered as selectivity site. Therefore, the moiety interacting with allosteric region was modified to improve the selectivity and activity. In this article, we attempted to develop novel Bcr-Abl inhibitors with enhanced biological activity.

It is well known that aniline containing halogen substituents (fluoro, chloro, bromo, and iodo) is useful for anti-cancer agents design. Halogen introduction can enhance the persistence and lipophilicity (6). Therefore, various halogen-substituted anilines were introduced to develop novel Bcr-Abl inhibitors. Meanwhile, some derivatives without halogen-substituted anilines were also prepared to validate the effect of halogen. Moreover, some heterocyclic amines and anilines containing tertiary amine side chain were incorporated to afford adequate structural diversity.

Chemistry

In this study, the title compounds were prepared from commercial available reagents (Scheme 1). One key intermediate (**5**) was yielded in high yield. The intermediate (**5**) was prepared in five steps. Firstly, carboxylate group of 3-amino-4-methylbenzoic acid (**1**) was protected by esterification with ethanol (**7**). Then, refluxing of compound (**2**) and acetonitrile in the presence of concentrated HCl afforded 3-guanidino-4-methylbenzoic acid ethyl ester nitrate (**3**) (**8**).

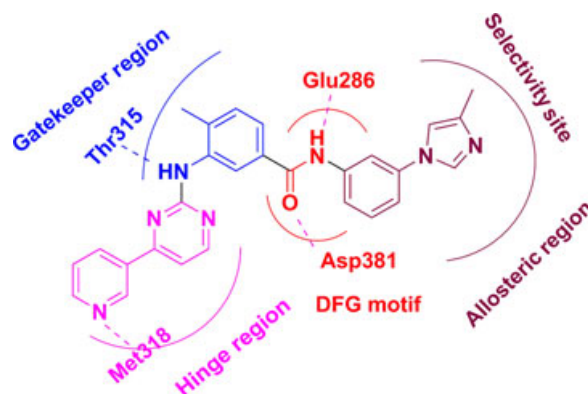
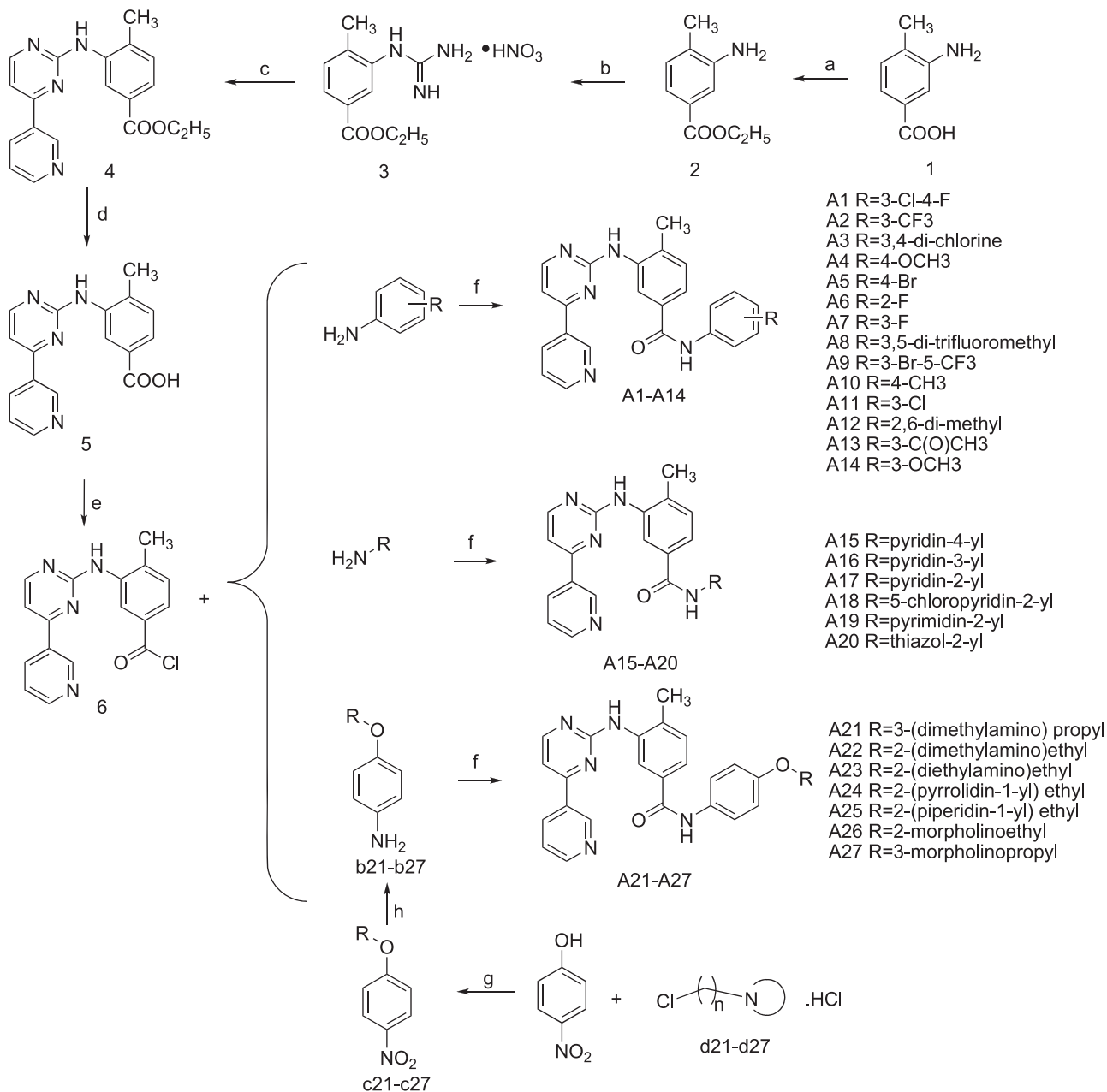


Figure 1: The interactions between Bcr-Abl kinase and inhibitors.



Scheme 1: Reagents and conditions: (a) EtOH, concd H₂SO₄, reflux; (b) H₂N-CN, concd HCl, EtOH, reflux, NH₄NO₃(aq); (c) 3-(dimethylamino)-1-(3-pyridinyl)prop-2-en-1-one, NaOH, n-BuOH, reflux; (d) NaOH, EtOH/H₂O(v:v = 1:1), 50 °C; (e) SOCl₂, DMF (cat), reflux; (f) substituted benzamides or substituted heterocyclic amines or compounds **b21–b27**, DIEA, DMAP (cat), DCM, r.t.; (g) Cs₂CO₃, DMF, 100 °C; (h) Pd/C, MeOH.

Compound (**4**) was afforded by reaction of 3-dimethylamino-1-(3-pyridinyl)-2-propen-1-one with compound (**3**) (**9**). The hydrolysis of (**4**) in NaOH aqueous solution yielded intermediate (**5**) (**10**). Finally, compound (**5**) was treated with SOCl₂ to form carbonyl chlorides and then reacted with various anilines to afford title compounds (**11**). Various heterocyclic aromatic amines were used in the synthesis of **A15–A20**. Twenty-seven 2-pyrimidinyl-amino-benzamides (**A1–A27**) were synthesized as novel Bcr-Abl inhibitors.

Experimental

Cell growth inhibition assays

Growth inhibitory activities were evaluated on K562 leukemia cancer cell lines. The effects of the compounds on cell viability were evaluated using the MTT assay. Exponentially growing cells were harvested and plated in 96-well plates at a concentration of 1 × 10⁴ cells/well and incubated for 24 h at 37 °C. The cells in the wells were, respectively,

treated with target compounds at various concentrations for 48 h. Then, 20 mL MTT (5 mg/mL) was added to each well and incubated for 4 h at 37 °C. After the supernatant was discarded, 150 mL DMSO was added to each well, and the absorbance values were determined by a microplate reader (Bio-Rad, Hercules, CA, USA) at 490 nm.

Kinase assays

The kinase inhibition assay and IC₅₀ determinations for wild-type Bcr-Abl were measured with the homogeneous time-resolved fluorescence (HTRF) KinEASE-TK assay from Cisbio according to the manufacturer's instructions. Wild-type Abl was purchased from Carma Biosciences, and 0.04 ng/ μ L kinase was used for test. ATP concentration was set at its K_m values (6.021 μ M), and 457.7 nM substrate was used. Kinase, substrate peptide, and inhibitors were added in 384-well plate, and then, reaction was started by addition of ATP. After completion of the reaction (30 min later), an antiphosphotyrosine antibody labeled with europium cryptate and streptavidin labeled with the fluorophore XL665 were added. The FRET between europium cryptate and XL665 was measured to quantify the phosphorylation of the substrate peptide. VICTOR X multilabel plate reader was used to measure the fluorescence of the samples at 620 nm (Eu-labeled antibody) and 665 nm (XL665-labeled streptavidin). The quotient of both intensities for reactions made with six different inhibitor concentrations (0.032–3.2 μ M, including no inhibitor) was plotted against inhibitor concentrations to determine IC₅₀ values. Each reaction was performed in duplicate, and at least two independent determinations of each IC₅₀ were made.

Chemistry: general procedures

All solvents and reagents were purified by standard techniques. Petroleum ether used refers to the fraction boiling in the range 60–90 °C. All reactions except those in aqueous media were carried out by standard techniques for moisture exclusion. Anhydrous reactions were carried out over dried glassware under nitrogen atmosphere. Reactions were monitored by TLC on 0.25-mm silica gel plates (60GF₂₅₄) and visualized with ultraviolet light. Melting points were obtained on electrothermal melting point apparatus and are uncorrected. ¹H-NMR spectra was recorded with a Bruker Advance 400 MHz instrument. Mass spectra were obtained on a Shimadzu GC-MS-QP2010 instrument.

3-Amino-4-methylbenzoic acid ethyl ester (2)

3-Amino-4-methylbenzoic acid (6.30 g, 41.72 mmol) was dissolved in 140 mL dehydrated ethanol. Under 0 °C, 4 mL concentrated H₂SO₄ was dropped to the above solution, and then, the solution was heated to reflux for 12 h. After the reaction was completed, ethanol was removed by reduced pressure distillation. Under 0 °C, 200 mL water was added, and the solution was adjusted to pH 6–7 with sodium bicarbonate. Then, the aqueous

was extracted with ethyl acetate (60 mL \times 2). The organic phase was combined and was washed by water (30 mL \times 2) and saturated sodium chloride (30 mL). The organic layer was dried over Na₂SO₄, filtered, and distilled under vacuum to give the crude product. The crude product was recrystallized by ether and EtOAc, giving a white solid (7.31 g). The total yield was 98%, mp 47–48 °C.

3-Guanidino-4-methylbenzoic acid ethyl ester nitrate (3)

In 100-mL round-bottomed flask, 3-amino-4-methylbenzoic acid ethyl ester (**2**) (3.00 g, 16.76 mmol) and cyanamide (1.68 g, 39.29 mmol) were added to ethanol (20 mL). While being stirred, concentrated HCl (2.16 mL, 25.41 mmol) was dropped slowly into the mixture. The mixture was heated to reflux for 15 h. Ethanol was removed by reduced pressure distillation, and water (20 mL) was added into the residue. Under 0 °C, NH₄NO₃ (2.70 g, 33.6 mmol) solution was dropped during 30 min. Then, the mixture was stirred for 30 min and filtered, giving the crude product. The crude product need to be purified by being washed with ether, and finally a white solid (4.66 g) was maintained. The total yield was 84.7%, mp 189–192 °C. EI-MS (m/z): 221.1 ([M]⁺-HNO₃).

4-Methyl-3-[[4-(3-pyridyl)-2-pyrimidinyl] amino] benzoic acid ethyl ester (4)

In a round-bottomed flask, 3-guanidino-4-methyl nitrate ethyl benzoate (**3**) (3.20 g, 11.26 mmol), 3-dimethylamino-1-(3-pyridyl)-2-propen-1-one (2.00 g, 11.26 mmol), and sodium hydroxide (0.54 g) were dissolved in *n*-butanol (20 mL). The mixture was stirred and heated to reflux for 72 h. Then, *n*-butanol was removed completely by reduced pressure distillation. EtOAc (50 mL) and water (30 mL) were added into the residue, and the mixture was stirred for 20 min. The organic phase was separated from the aqueous phase, and the aqueous phase was extracted by EtOAc (20 mL \times 2). The combined organic phase was washed by water (15 mL) and saturated sodium chloride (15 mL). The organic layer was dried over Na₂SO₄, filtered, and distilled under vacuum to give the crude product. The crude product was recrystallized by ether and EtOAc, giving a white solid (2.76 g). The total yield was 73.4%, mp 91–92 °C. EI-MS (m/z): 334.1 [M]⁺. ¹H NMR (400 MHz, CDCl₃): δ = 1.40 (t, J = 7.20 Hz, 3H), 2.41 (s, 3H), 4.41 (q, J = 7.20 Hz, 14.00 Hz, 4H), 7.12 (s, 1H), 7.24 (d, J = 4.0 Hz, 1H), 7.28–7.32 (m, 2H), 7.46 (s, 1H), 7.75 (dd, J = 4.0 Hz, 8.0 Hz, 1H), 8.45 (d, J = 8.0 Hz, 1H), 8.54 (d, J = 8.0 Hz, 1H), 8.93 (s, 1H).

4-Methyl-3-[[4-(3-pyridyl)-2-pyrimidinyl] amino] benzoic acid (5)

In a 250-mL flask, 4-methyl-3-[[4-(3-pyridyl)-2-pyrimidinyl] amino] ethyl benzoate (**4**) (5.18 g, 15.5 mmol) was dissolved into the mixed solution of ethanol/water (60/

60 mL). While being stirred, NaOH (2 M, 25 mL) was dropped in the mixture. Then, the mixture was heated to 45–50 °C and was maintained at this temperature for 4 h. Ethanol was removed by reduced pressure distillation, and then, EtOAc (20 mL) was added. Then, the organic phase was abandoned. The aqueous phase was adjusted to pH 7–8 using HCl (2 M), and yellow solid was precipitated. The suspension was filtered, giving the crude product (4.10 g). The total yield was 87%, mp 258–260 °C. EI-MS (m/z): 306.1 [M]⁺. ¹H NMR (400 MHz, DMSO-*d*₆): δ = 2.31 (s, 3H), 7.12 (s, 1H), 7.30 (d, *J* = 8.0 Hz, 1H), 7.52 (d, *J* = 4.0 Hz, 1H), 7.60–7.66 (m, 3H), 8.30 (s, 1H), 8.57 (d, *J* = 4.0 Hz, 2H), 8.76 (s, 1H), 9.13 (s, 1H), 9.32 (s, 1H).

4-Methyl-3-[[4-(3-pyridyl)-2-pyrimidinyl] amino] benzoyl chloride (6)

In a 50-mL flask, 4-methyl-3-[[4-(3-pyridyl)-2-pyrimidinyl] amino] benzoic acid (**5**) (0.96 g, 3.14 mmol) was added in anhyd SOCl₂ (10 mL). Then, in the suspension, DMF was added 3–4 drops. The mixture was heated to reflux for 1.5 h. Then, SOCl₂ was removed completely by reduced pressure distillation. The residue was reserved for the next step.

***N*-(3-chloro-4-fluorophenyl)-4-methyl-3-(4-(pyridin-3-yl)pyrimidin-2-ylamino)benzamide (A1)**

In a 50 mL flask, 4-methyl-3-[[4-(3-pyridyl)-2-pyrimidinyl] amino] benzoyl chloride (**6**) was dissolved into CH₂Cl₂ (20 mL). Under 0 °C, the CH₂Cl₂ (10 mL) solution of 3-Chloro-4-fluoroaniline (0.46 g, 3.14 mmol), *N,N'*-diisopropyl ethylamine (4.0 mL) and 4-(dimethylamino) pyridine (cat.) was dropped slowly into the above suspension. After that, the mixture was reacted at r.t. overnight. The mixture was diluted with CH₂Cl₂ (20 mL), and was washed with saturated NaCl solution (10 mL × 2), saturated NaHCO₃ solution (10 mL × 3), water (10 mL × 2). Then the organic phase was dried by Na₂SO₄, and filtered, giving the crude product. The crude product was purified by chromatography (ethyl acetate:methanol = 5:1), giving a solid (0.36 g). The total yield was 27%. Mp 196–198 °C, EI-MS (m/z): 432.9[M]⁺, ¹H NMR (400 MHz, CDCl₃): δ = 2.21 (s, 3H), 7.12–7.56 (m, 4H), 7.69 (s, 1H), 7.88 (d, *J* = 8.0 Hz, 1H), 8.24 (d, *J* = 8.0 Hz, 1H), 8.43 (d, *J* = 8.0 Hz, 1H), 8.56 (d, *J* = 4.0 Hz, 1H), 8.64 (d, *J* = 4.0 Hz, 1H), 8.85 (s, 1H), 9.19 (s, 1H), 9.30 (s, 1H), 10.18 (s, 1H).

Compounds **A2–A14** were prepared using the general procedure described above.

4-Methyl-3-(4-(pyridin-3-yl) pyrimidin-2-ylamino)-*N*-(pyridin-4-yl) benzamide (A15)

In a 50-mL flask, 4-methyl-3-[[4-(3-pyridyl)-2-pyrimidinyl] amino] benzoyl chloride (**6**) and pyridin-4-amine (0.35 g, 3.72 mmol) was dissolved into CH₂Cl₂ (20 mL). Under

0 °C, the CH₂Cl₂ (10 mL) solution of *N,N'*-diisopropyl ethylamine (4.0 mL) and 4-(dimethylamino) pyridine (cat) was dropped slowly into the above suspension. After that, the mixture was reacted at r.t. overnight. The mixture was diluted with CH₂Cl₂ (20 mL) and was washed with saturated NaCl solution (10 mL × 2), saturated NaHCO₃ solution (10 mL × 3), and water (10 mL × 2). Then, the organic phase was dried by Na₂SO₄ and filtered, giving the crude product. The crude product was purified by chromatography (ethyl acetate: methanol = 3:1), giving a solid (0.68 g). The total yield was 56.7%.

Mp 234–237 °C, EI-MS (m/z): 382.1[M]⁺, ¹H NMR (400 MHz, CDCl₃): δ = 2.46 (s, 3H), 7.26 (d, *J* = 4.0 Hz, 1H), 7.36–7.38 (m, 3H), 7.44–7.46 (m, 1H), 7.60 (d, *J* = 8.0 Hz, 1H), 8.29 (s, 1H), 8.39–8.46 (m, 3H), 8.55 (d, *J* = 4.0 Hz, 1H), 8.74–8.75 (m, 2H), 8.85 (s, 1H), 9.29 (s, 1H).

Compounds **A16–A20** were prepared using the general procedure described above.

***N,N*-dimethyl-3-(4-nitrophenoxy) propan-1-amine (c21)**

In 100-mL flask, 4-nitrophenol (1.39 g, 10 mmol) was dissolved in 20 mL anhydrous DMF. Then, 3-chloro-*N,N*-dimethylpropan-1-amine hydrochloride (**d21**) (1.57 g, 10 mmol), and Cs₂CO₃ (5.29 g, 15 mmol) were added to the solution. Under N₂, the mixture was heated to 100 °C and was reacted for 2.5 h. The mixture was filtered, and the filtrate was poured to ice water (200 mL). The aqueous phase was extracted by EtOAc (30 mL × 3). The combined organic phase was washed by Na₂CO₃ (10 mL × 4), water (10 mL × 2), and saturated sodium chloride (15 mL). The organic layer was dried over Na₂SO₄ to give the crude product.

4-(3-(Dimethylamino) propoxy) benzenamine (b21)

N,N-dimethyl-3-(4-nitrophenoxy) propan-1-amine (**c21**) (3.92 mmol) was dissolved in 30 mL anhydro-methanol, and then, 0.1 g Pd/C(5%) was added to this solution. After that, the mixture was reacted at r.t. under N₂ for 4 h. The mixture was filtered, and Pd/C was washed with methanol for 3–4 times. The organic phases were combined, and methanol was removed by reduced pressure distillation to give the crude product. The residue was reserved for the next step.

Compounds **b21–b27** were prepared using the general procedure described above.

***N*-(4-(3-(dimethylamino)propoxy) phenyl)-4-methyl-3-(4-(pyridin-3-yl) pyrimidin-2-ylamino) benzamide (A21)**

In a 50-mL flask, 4-methyl-3-[[4-(3-pyridyl)-2-pyrimidinyl] amino] benzoyl chloride (**6**) was dissolved into CH₂Cl₂

(20 mL). Under 0 °C, the CH₂Cl₂ (10 mL) solution of 4-(3-(dimethylamino) propoxy)benzenamine (**b21**) (3.92 mmol), *N,N'*-diisopropyl ethylamine (5.0 mL), and 4-(dimethylamino) pyridine (cat) was dropped slowly into the above suspension. After that, the mixture was reacted at r.t. overnight. The mixture was diluted with CH₂Cl₂ (20 mL) and was washed with saturated NaCl solution (10 mL × 2) and saturated NaHCO₃ solution (10 mL × 3). Then, the organic phase was dried by Na₂SO₄ and filtered, giving the crude product. The crude product was purified by chromatography (ethyl acetate: methanol = 1:1), giving a solid (0.52 g). The total yield was 34%, mp 133–136 °C, EI-MS (*m/z*): 437.3[M-NC₂H₆+H]⁺; ¹H NMR (400 MHz, CDCl₃): δ = 2.29–2.33 (m, 2H), 2.45 (s, 3H), 2.74 (s, 6H), 3.09 (t, *J* = 8.0 Hz, 2H), 4.07 (t, *J* = 6.0 Hz, 2H), 6.88 (d, *J* = 8.0 Hz, 2H), 7.25 (d, *J* = 4.0 Hz, 1H), 7.35 (d, *J* = 8.0 Hz, 1H), 7.41–7.44 (m, 1H), 7.57 (d, *J* = 8.0 Hz, 3H), 7.98 (s, 1H), 8.44 (d, *J* = 8.0 Hz, 1H), 8.55 (d, *J* = 8.0 Hz, 1H), 8.74 (d, *J* = 4.0 Hz, 1H), 8.81 (s, 1H), 9.27 (s, 1H).

Compounds **A22–A27** were prepared using the general procedure described above.

The melting point and spectral data of compounds (**A2–A14**, **A16–A20**, and **A22–A27**) are provided as Appendix S1 and S2.

Results and Discussion

All the title compounds were evaluated for their Bcr-Abl inhibitory activity (12). The results were summarized in Tables 1, 2 and 3. Most of them exhibited potent Bcr-Abl inhibitory activity. Compound (**A26**) was the most potent with IC₅₀ value of 10.15 nM. Moreover, four compounds (**A2**, **A8**, **A9**, and **A19**) were also potent Bcr-Abl inhibitors with IC₅₀ values ranging from 135.56 to 258.57 nM. These

Table 1: Structure and activity of **A1–A14**

Compounds	R	Bcr-Abl IC ₅₀ (μM)	K562 cells IC ₅₀ (μM)
A1	3-Cl-4-F	9.569	0.407
A2	3-CF ₃	0.136	2.167
A3	3,4- <i>di</i> -Cl	1.513	0.391
A4	4-OCH ₃	0.924	5.855
A5	4-Br	0.483	0.439
A6	2-F	0.569	5.934
A7	3-F	1.069	6.404
A8	3,5- <i>di</i> -CF ₃	0.259	0.218
A9	3-Br-5-CF ₃	0.219	0.258
A10	4-CH ₃	1.105	1.984
A11	3-Cl	ND ^a	1.283
A12	2,6- <i>di</i> -CH ₃	0.956	0.704
A13	3-C(O)CH ₃	0.542	4.370
A14	3-OCH ₃	5.243	16.783
Nilotinib	–	0.214	3.538

^aND is not determined.

Table 2: Structure and activity of **A15–A20**

Compounds	R	Bcr-Abl IC ₅₀ (μM)	K562 cells IC ₅₀ (μM)
A15		2.190	88.682
A16		4.025	10.274
A17		3.578	260.148
A18		0.305	6.087
A19		0.210	23.957
A20		3.578	5.936
Nilotinib	–	0.214	3.538

Table 3: Structure and activity of **A21–A27**

Compounds	R	Bcr-Abl IC ₅₀ (μM)	K562 cells IC ₅₀ (μM)
A21		13.193	2.162
A22		20.998	6.332
A23		>100	2.273
A24		>100	17.262
A25		>100	2.621
A26		0.010	26.906
A27		>100	10.695
Nilotinib	–	0.214	3.538

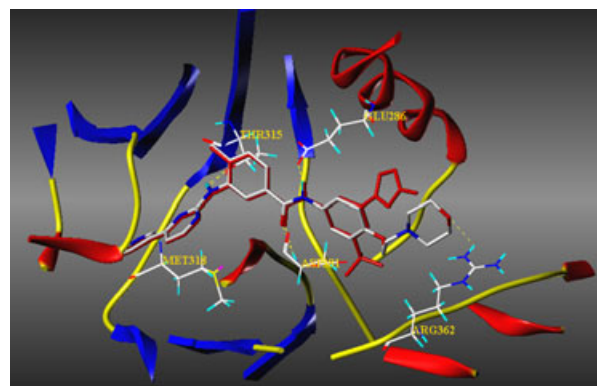
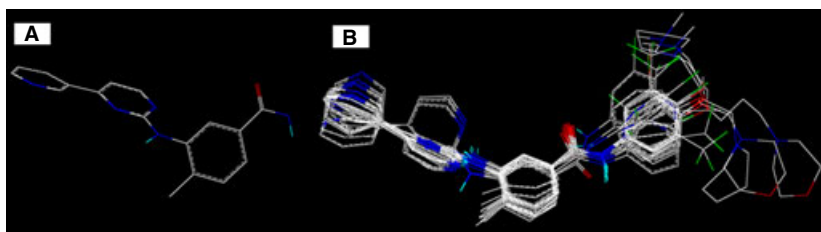


Figure 2: Binding mode of nilotinib (red) and **A26** with Bcr-Abl.

compounds could be considered as promising candidates for the development of novel Bcr-Abl inhibitors.

All the compounds were evaluated for antitumor activities against Bcr-Abl positive leukemia cell (K562). Most of them

Figure 3: (A) Structure A; (B) Superposition of 18 inhibitors for CoMFA construction.



exhibited potent antiproliferative activity. In particular, compounds (**A8**) and (**A9**) displayed potent activities with IC_{50} values of 217.65 and 258.32 nM, respectively. Five compounds (**A1**, **A3**, **A5**, **A12**, and **A18**) were more potent than nilotinib. The anticancer activities of **A2**, **A10**, **A11**, **A21**, **A22**, and **A25** were comparable with that of nilotinib.

As shown from Table 1, compounds with halogen-substituted anilines were more potent than the others. It was suggested that incorporation of halogen could improve their biological activity. The results indicated that halogen played important role in Bcr-Abl inhibitory activity. Higher potency of **A2**, **A8**, and **A9** indicated that trifluoromethyl group may be of benefit to anticancer activity.

The biological activities of **A15–A20** were listed in Table 2. Replacement of anilines with heterocyclic aromatic amines led to reduction in activity. Compound **A18** was more potent than **A17**, which suggested that incorporation of halogen into heterocyclic amines could improve Bcr-Abl inhibitory activity and antitumor effects. Moreover, **A19** displayed similar Bcr-Abl inhibitory activity compared with nilotinib and could be considered as a novel lead compound for further optimization.

As shown in Table 3, **A21–A23** displayed potent antiproliferative activity against K562 cells. However, **A24**, **A25**, and **A27** exhibited poor Bcr-Abl inhibitory activity. Surpris-

ingly, **A26** was more potent than nilotinib, exhibiting excellent inhibitory activity against Bcr-Abl kinase. It might be considered as a potent Bcr-Abl inhibitor.

Docking and SAR Studies

Docking

To investigate the interactions between inhibitors and Bcr-Abl, molecular docking was carried out using Surflex-Dock Mode of SYBYL-X 2.0 program package (Tripos, St. Louis, MO, USA). The small molecules and the X-ray crystal structure of Bcr-Abl (PDB ID: 3CS9) were imported. Nilotinib was used to define the binding cavity (13). All compounds were used to perform docking, and the docking result of **A26** was shown in Figure 2. It binds to active site of Bcr-Abl in a similar fashion to that of nilotinib. It interacts with receptor through five hydrogen bonds involving the pyridyl-N and the backbone NH of Met-318, the anilino-NH and the OH of Thr-315, the amido-NH and side chain carboxylate of Glu-286, the amido carbonyl and the backbone NH of the Asp-381 and the morpholine-O with side chain guanidyl of Arg-362.

QSAR studies

3D-QSAR studies were performed with CoMFA module of SYBYL-X 2.0. The test set consisted of nilotinib, **A6**, **A8**,

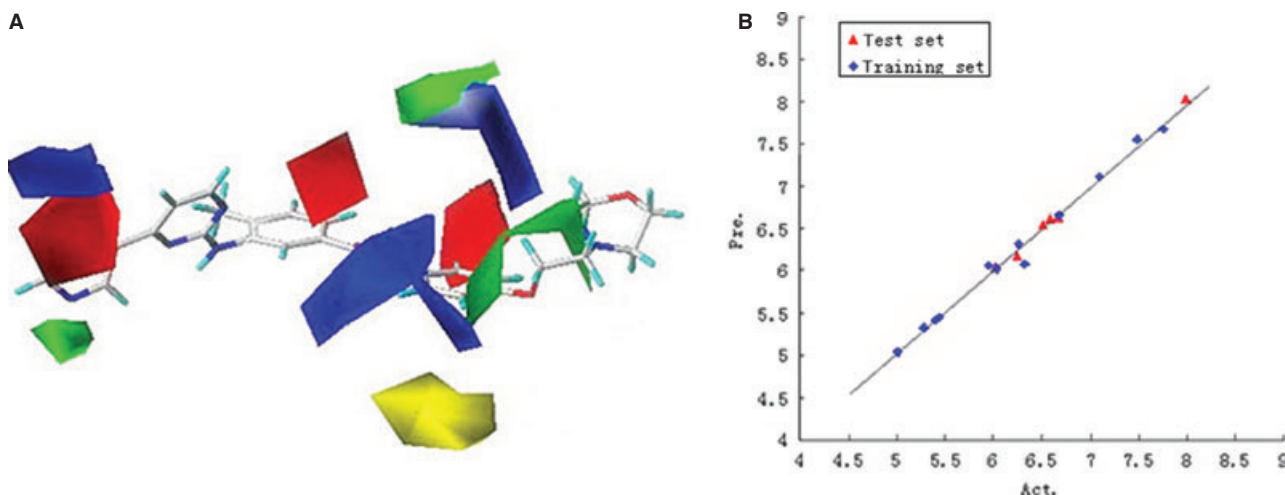


Figure 4: (A) The most active molecule **A26** is shown in the background. Red color represents the negative charge region, blue is the positive charge region, green is the more bulky region, and yellow is the less bulky region. (B) the predictability of the CoMFA model.

A14, A17, and A26, the other **18** compounds (**A1, A4–A6, A8, A10, A12, A14–A20, A24, A26, and A27**) composed of the training set. The IC_{50} values were converted into pIC_{50} according to the formula: $pIC_{50} = \log_{10}IC_{50}$.

The conformations of training set generated from docking study were used. Based on the docking results, the template molecule nilotinib was taken and the others were aligned to it using structure A as scaffold by DATA-BASE ALIGNMENT method in the SYBYL-X 2.0. The aligned molecules are shown in Figure 3.

The steric and electrostatic fields were calculated at each lattice intersection of regularly spaced grid of 2.0 Å in all three dimensions within defined region. An sp^3 carbon atom with +1.00 charge was used as a probe atom. The steric and electrostatic fields were truncated at +30.00 kcal/mol, and the electrostatic fields were ignored at the lattice points with maximal steric interactions.

PLS method was used to linearly correlate CoMFA fields with activity values. The cross-validation analysis was performed using leave-one-out (LOO) method. The cross-validated q^2 (0.568) that resulted in optimum number of components ($n = 7$) and lowest standard error of prediction were considered for further analysis. We have evaluated different filter value σ and at least selected σ as 2.00 kcal/mol to speed up the analysis and reduce noise. As described in Figure 4(A), red color represents the negative charge region, blue is the positive charge region, green is the more bulky region, and yellow is the less bulky region.

The LOO cross-validated q^2 of the CoMFA model is 0.569, and the non-cross-validated r^2 for the model established by the study is 0.992. The value of the variance ratio F ($n_1 = 7, n_2 = 10$) is 170.457, and standard error of the estimate (SEE) is 0.099. The contribution of electrostatic and steric is 63.3% and 36.7%, respectively. From Figure 4(B), we can find that the CoMFA model can predict test set compounds (**1, A6, A8, A14, A17, and A26**) well.

Conclusions

In this study, a series of novel Bcr-Abl inhibitors was designed and synthesized. The moiety interacting with allosteric region of Bcr-Abl was modified to improve the selectivity and biological activity. Most of them exhibited potent Bcr-Abl inhibitory activity and antiproliferation against K562 cells. The results indicated that incorporation of halogenated-aniline or anilines containing tertiary amine moiety could improve Bcr-Abl inhibitory activity and antitumor effects. Moreover, the 3D-QSAR studies of these compounds gave a contribution to the exploration of Bcr-Abl inhibitors' structure–activity relationship.

Acknowledgment

This work was supported by the National Natural Science Foundation (NNSF) of China (Grant No. 81302737, 81302641, and 81230079), the Fundamental Research Funds for the Central Universities, and Natural Science Basic Research Plan in Shaanxi Province of China.

Reference

1. Yao J., Chen J., He Z., Sun W., Xu W. (2012) Design, synthesis and biological activities of thiourea containing sorafenib analogs as antitumor agents. *Bioorg Med Chem*;20:2923–2929.
2. Boschelli D.H. (2007) Bcr-Abl Kinase inhibitors. *Top Med Chem*;1:407–444.
3. Deininger M.W. (2008) Nilotinib. *Clin Cancer Res*;14: 4027–4031.
4. Weisberg E., Manley P., Mestan J., Cowan-Jacob S., Ray A., Griffin J.D. (2006) AMN107 (nilotinib): a novel and selective inhibitor of BCR-ABL. *Br J Cancer*;94:1765–1769.
5. Dietrich J., Hulme C., Hurley L.H. (2010) The design, synthesis, and evaluation of 8 hybrid DFG-out allosteric kinase inhibitors: a structural analysis of the binding interactions of Gleevec, Nexavar, and BIRB-796. *Bioorg Med Chem*;18:5738–5748.
6. Pizzirani D., Roberti M., Grimaudo S., Di Cristina A., Pipitone R.M., Tolomeo M., Recanatini M. (2009) Identification of biphenyl-based hybrid molecules able to decrease the intracellular level of Bcl-2 protein in Bcl-2 overexpressing leukemia cells. *J Med Chem*;52:6936–6940.
7. Zhai Z.W., Yang S.H. (2010) Improvement of the synthetic technology of methyl (ethyl) m-aminobenzoate. *App Chem Ind*;39:1437–1442.
8. Gao Y.J., Gao H.X., Lu R.H. (2003) Progressing in the synthesis of guanidines. *J Chin Syn Chem*;11: 193–202.
9. Bennett G.B., Mason R.B., Alden L.J., Roach J.B. Jr (1978) Synthesis and anti-inflammatory activity of tri-substituted pyrimidines and triazines. *J Med Chem*;21: 623–628.
10. Tang J., Duan T.H., Li M.H. (1988) Synthesis of (6, 8-disubstituted coumarin-3-formamido) - cephalosporins. *J China Pharm Univ*;19:253–257.
11. Pan X., Lu W., Li P., Wang F., Wang C., Hu Z., Zhang J. (2012) A novel and facile synthetic approach for tassigna. *Med Chem*;8:985–989.
12. Jia Y., Quinn C.M., Gagnon A.I., Talanian R. (2006) Homogeneous time-resolved fluorescence and its applications for kinase assays in drug discovery. *Anal Biochem*;356:273–281.
13. Weisberg E., Manley P.W., Breitenstein W., Bruggen J., Cowan-Jacob S.W., Ray A., Huntly B. *et al.* (2005) Characterization of AMN107, a selective inhibitor of native and mutant Bcr-Abl. *Cancer Cell*;7:129–141.



Supporting Information

Additional Supporting Information may be found in the online version of this article:

Appendix S1. Melting points and spectral data of compounds (A2–A14, A16–A20, A22–A27).

Appendix S2. GC-MS and ^1H NMR of compounds A1–A27.